Research Square

Preprints are preliminary reports that have not undergone peer review.
They should not be considered conclusive, used to inform clinical practice,
or referenced by the media as validated information.

Cabozantinib reshapes the CD4+ T-cell exhaustion program in clear cell renal cell carcinoma through multi-target kinase inhibition and cytokine remodeling

Piotr Domanski
The Maria Sklodowska-Curie National Research Institute of Oncology
Małgorzata Stachowiak
The Maria Sklodowska-Curie National Research Institute of Oncology
Natalia Rusetska
The Maria Sklodowska-Curie National Research Institute of Oncology
Agnieszka Świć
The Maria Sklodowska-Curie National Research Institute of Oncology
Daniel Bajerski
The Maria Sklodowska-Curie National Research Institute of Oncology
Maciej Łuba
The Maria Sklodowska-Curie National Research Institute of Oncology
Sergiusz Markowicz
The Maria Sklodowska-Curie National Research Institute of Oncology
Jakub Kucharz
The Maria Sklodowska-Curie National Research Institute of Oncology
Paweł Wiechno
The Maria Sklodowska-Curie National Research Institute of Oncology
Elzbieta Sarnowska
elzbieta.sarnowska@nio.gov.pl

The Maria Sklodowska-Curie National Research Institute of Oncology

Article

Keywords: CD4 + T-cell exhaustion, AXL expression, cabozantinib, ccRCC

Posted Date: September 8th, 2026

DOI: https://doi.org/10.21203/rs.3.rs-10750161/v1

License: This work is licensed under a Creative Commons Attribution 4.0 International License.
Read Full License

Additional Declarations: No competing interests reported.

Abstract

Clear cell renal cell carcinoma (ccRCC) is a highly immunogenic malignancy, yet the contribution of exhausted CD4+ T-cells to therapeutic response remains poorly understood. We investigated whether cabozantinib, a multi-kinase inhibitor used in metastatic ccRCC, modulates the dysfunctional state of tumor-conditioned CD4+ T-cells. In a human co-culture model with 786-O cells, exhausted CD4+ T-cells displayed marked induction of AXL, together with upregulation of key exhaustion-associated molecules. Cabozantinib suppressed *AXL*, *CD274*, and other gene expression at the transcript level and reduced total PD-1 and PD-L1 protein abundance, while exerting no measurable effect on CD+ T-cell yield. Functionally, cabozantinib attenuated the inflammatory program of exhausted CD4+ T-cells by reducing IL-1β and IL-6 expression and secretion and by reshaping the extracellular cytokine milieu. This effect was accompanied by increased TGFβ2 and IDO1 expression, indicating immune reprogramming rather than simple restoration of effector function. In clinical specimens, AXL was detected in both tumor cells and TILs in ccRCC. Additionally, patients with metastatic RCC treated with cabozantinib exhibited reduced systemic inflammatory indices during therapy. Together, these findings identify AXL-associated exhausted CD4+ T-cells as a previously underappreciated target of cabozantinib and highlight CD4+ T-cell reprogramming as a potential component of its immunomodulatory activity in ccRCC.

1. Introduction

Renal cell carcinoma (RCC) is the most commonly diagnosed solid lesion in the kidney and accounts for 90% of all kidney malignancies [1] and contributes to around 2% of cancer-related deaths worldwide [2]. Clear cell RCC (ccRCC) represents around 70% of all RCC histological subtypes, which usually develop on a background of different sporadic mutations including VHL mutation [3]. Şenbabaoğlu et al. investigated the immunogenicity of epithelial tumors and reported that ccRCC has the highest overall T-cell, CD8 + T-cell, CD4 + T-cell (Th1), dendritic cell (DC), neutrophil, and relatively low CD4 + T-cell Th2 and regulatory T-cell scores, which suggests an proinflammatory profile [4]. Therefore, the use of immunotherapy in the treatment of RCC has proved reasonable and effective, prolonging both progression-free survival (PFS) and overall survival (OS). A comprehensive investigation into the tumor-immune system interactions could provide significant benefits to patients. For instance, the process of reversing T-cell exhaustion and restoring full cytotoxic capacity can increase the effectiveness of treatment.

The function of CD4 + T-cells remains to be fully elucidated, as numerous studies have focused more on the anti-tumor activity of CD8 + T-cells. However, CD4 + T-cells regulate CD8 + T-cells activity and are crucial in response to immunotherapy, which prompts us to investigate exhaustion-related processes and potential ways to reverse exhaustion [5,6]. A number of studies have indicated that the absence of CD4 + T-cells impedes the complete activation of CD8 + T-cells, resulting in anergy and lack of CD8 + memory T-cells [7,8]. Moreover, CD4 + T-cells possess the capacity to induce cytotoxicity through the production of IFN-γ and TNF-α and also by the expression of ligands such as FasL and TRIAL [9].

Furthermore, studies in mice show that CD4 + T-cells can even eliminate tumor cells resistant to CD8 + T-cells, even without expression of major histocompatibility complex (MHC) class II [10]. Therefore, subsequent investigation of the factors such as CD4 + T-cell cytotoxicity, exhaustion mechanisms, and differentiation towards particular Th classes may prove beneficial.

Jancewicz et al. conducted a detailed study of CD4 + T-cell exhaustion using kidney and breast cancer cell lines and reported significant elevations in proangiogenic factors as well as pro-inflammatory cytokines such as IL-1β and IL-6 [6]. The findings, along with the outcomes of clinical trials, demonstrated that the combination of Vascular Epithelial Growth Factor Receptor-Tyrosine Kinases Inhibitors (VEGFR-TKIs) and Immune Checkpoint Inhibitors (ICIs) could enhance the therapeutic efficacy [11]. Sunitinib was among the first TKIs to be used instead of IFN-α and IL-2 therapies. The median PFS of the registration trial was significantly longer for sunitinib compared to IFN-α [12]. Acceptable treatment tolerance and efficacy led to the introduction of further TKIs such as cabozantinib, that inhibit multiple receptors and kinases including MET, AXL, RET, and VEGFR2. This multi-targeted mechanism appears to underlie its immunomodulatory properties, making it a notable drug among the VEGFR-TKIs used in RCC treatment. This profile of inhibition affects the tumor physiology and leads to tumor cell apoptosis, vascular disruption, and escalation of intratumoral hypoxia, making the tumor more susceptible to immune-mediated elimination [13–16]. However, these studies do not refer to CD4 + T-cells and the exhaustion mechanism, which seems to be crucial in the prolonged state of heightened immune system stimulation that is characteristic of the cancer process.

In this study, we show the potential of VEGFR-TKI cabozantinib to decrease pro-inflammatory cytokines, such as IL-1β and IL-6, in exhausted CD4 + T-cells, and to influence the tumor immune-microenvironment. Consequently, this may result in a reduction of the immunosuppressive effect. Additionally, the present study indicates that sunitinib and cabozantinib have the potential to decrease PD-L1 expression, a hallmark of exhausted and anergic CD4 + T-cells [6]. In addition, significantly elevated AXL expression was observed in tumor infiltrating lymphocytes (TILs) in ccRCC samples, which has been identified as a therapeutic target for cabozantinib. This prompts further examination into the potential role of AXL in T-cell exhaustion and its potential as a therapeutic target for reversing this process. The described components and enhanced infiltration of TILs may provide a mechanistic explanation for the synergistic effect of VEGFR-TKIs with ICIs reported in clinical trials [11].

2. Materials and methods

2.1. Cancer cell culture

The 786-O, RRID:CVCL_1051 (ATCC) clear cell renal cell carcinoma cell line was in the possession of Maria Sklodowska-Curie National Research Institute of Oncology. The cells were cultured in RMPI (Biowest, no. cat L0500), supplemented with 10% heat-inactivated fetal bovine serum, FBS (Biowest, no.

cat S181H-500). Culture was maintained in standard conditions, at 37°C, 5% CO_2 and humidified atmosphere. Prior to experiments, the cells were tested for mycoplasma contamination.

2.2. CD4 + T-cell culture

Blood from healthy male donors under the age of 35 years was obtained from Regional Blood Center in Warsaw. Blood was centrifuged on a Ficoll-Paque (Cytiva, no. cat 17144002) gradient to obtain peripheral blood cells (PBMC), followed by multiple 0.9% NaCl washes to reduce the platelet concentration. The cells were counted, resuspended in AIM-V (Gibco no. cat 12055083) medium, and plated on plastic plates to separate adherent and non-adherent-cells. The cells were transferred to Teflon® vessels for overnight incubation under standard culture conditions. Isolated PBMCs were counted and subjected to CD4 + T-cell isolation using negative isolation kits (Dynabeads Untouched CD4 + Isolation, Invitrogen, no. cat 11346D) according to the manufacturer's protocol. Subsequently, CD4 + T-cells were stimulated with anti-CD2/CD3/CD28-coated magnetic beads (Miltenyi Biotec, no. cat 130-091-441), supplemented with 10 U/ml hIL-2 (Miltenyi Biotec, no. cat 130-097-743), and cultured at 0,5 x 10^6 cells/ml density in AIM-V at standard conditions for 12 days. The cells were divided 1/3 every 3- to 4-day intervals, with fresh medium with 10 U/ml IL-2.

2.3. Co-culture of cancer cells and CD4 + T-cells with drug treatment

Following the initial round of stimulation, the cells were restimulated on day 12 and cultured for 72 hours in the presence (T15 group) or absence (TNT group) of cancer cells. The groups were subjected to treatment with selected concentrations of DMSO (~ 0.1% final) or cabozantinib (7 μM final). The drug concentration were selected through previous experimental determination based on the results of MTT tests conducted on both CD4 + T-cells and tumor cells. Subsequent to 3-day incubation, the CD4 + T-cells were divided into smaller portions for further downstream applications.

2.4. Flow cytometry

At least 0,35 x 10^6 CD4 + T-cells were separated for the subsequent flow cytometric analysis. In accordance with the standard protocol, cells were first subjected to a thorough washing process with Phosphate Buffered Saline (PBS) and then incubated with LIVE/DEAD™ Fixable Blue Dead Cell Stain Kit (Invitrogen, no. cat L23105). Thereafter, the cells were thoroughly washed with FACS buffer (PBS with 1% FBS), and then stained with fluorophore-conjugated antibodies diluted in the same buffer (Suppl. Data S2.). Following a one-hour incubation period at 4°C, the stained cells underwent a series of washes with FACS buffer. Thereafter, they were fixed with 1% paraformaldehyde, thoroughly washed again, and resuspended in fresh FACS buffer for the subsequent analysis by flow cytometry. The flow cytometry procedure was carried out at the MSCNRIO, employing the BD FACS Aria III from Becton Dickinson. The subsequent data analysis was conducted using the FlowJo™ Software (RRID: SCR_008520).

2.5. Western blot

Preliminary to conducting Western blot analysis, SDS-PAGE was performed. The separation gel contained 2,2,2-trichloroethanol (TCE, Sigma-Aldrich, no. cat 8.08610) at a final concentration of 0.5%, which facilitated the visualization of proteins at a wavelength of 302 nm [17]. Precision Plus Protein Dual Color Standards (BIO-RAD, no. cat 1610394) was used as molecular weight marker. The protein extract, obtained from 2.5-5 x 10^6 cells, was resuspended in Laemmli Buffer and heated to 95°C. A portion of the obtained lysate was applied to the gel, and electrophoresis was carried out in a vertical electrophoresis system (BIO-RAD) at a constant voltage of 130 V for approximately 1.5 hours. Subsequently, the bands obtained after electrophoretic separation were subjected to visualization using a transilluminator with UV (λ = 305 nm) to ascertain the protein loading control. The protein transfer process was carried out on a PVDF membrane with pores measuring 0,45 µm (Millipore, no. cat IPFL85R). The transfer was conducted in TBE buffer (0.13 M Tris-base, 45 mM boric acid), with a constant voltage of 70 V applied for a duration of 2 hours with cooling. Subsequently, UV illumination was utilized to visualize the bands on the membrane, confirming the successful transfer. Following this, the membrane was blocked for 1 hour at ambient temperature using a 5% skimmed milk in TBS-T (TBS + 0,1% Tween-20) buffer. The membrane was then incubated overnight at 4°C with primary antibodies specific for the antigen of interest (Suppl. Data S2.), which had been suspended in a suitable dilution in 5% skimmed milk or 5% BSA (BioShop, no. cat ALB001.250). The following day, the membrane was washed 3 x 5 min in TBS-T buffer and incubated with the appropriate secondary antibody conjugated to HRP, diluted in 5% milk in TBS-T. Subsequent washes were then performed before applying WesternBright™ Quantum (Advansta Inc.) to the membrane. The resultant light signal was collected and documented using imaging system Amersham™ brand ImageQuant™ 800 (Cytiva). Uncropped and unedited gels and membranes can be found in Suppl. Data S1.

2.6. Quantitative Real Time PCR (qRT-PCR)

Total RNA was isolated using a ready-to-use ReliaPrep™ RNA Miniprep Systems kit (Promega, no. cat Z6014). A total of 5 x 10^6 cells were harvested for isolation of RNA from CD4 + T-cells. The entire process was performed in strict accordance with the manufacturer's protocol. Complementary DNA (cDNA) was prepared from 1 µg of total RNA using the Transcriptor First Strand cDNA Synthesis Kit (Roche, no. cat 04379012001) according to the instructions. cDNA was diluted 10x and used as a qRT-PCR template. The reactions incorporated iTaq Universal SYBR Green Supermix (BIO-RAD, no. cat 1725124) and primers designed to target the gene of interest (Suppl. Data S2.). Ubiquitin was utilized as a reference gene. The results were analyzed using the 2^(-ΔΔCT) method, as outlined in the publication by Rao et al. (2013) [18].

2.7. Cytokine assay

Supernatants (1000 µl) collected from each of the lymphocyte groups after co-culture experiment were used to detect cytokines released by cells into the medium using the ready-to-use Proteome Profiler Human Cytokine Array Kit (R&D Systems, no. cat ARY006), according to the protocol provided by the manufacturer. Briefly, nitrocellulose membranes were coated by specific antibodies in duplicates. The captured proteins were then detected by biotinylated detection proteins conjugated with HRP

(streptavidin-HRP), and chemiluminescence detection reagents were used to visualize the results. The signal (pixel density) was proportional to the amount of bound analyte. Signal reading was determined using Amersham™ brand ImageQuant™ 800 (Cytiva). Mean pixel density was calculated using ImageJ software (RRID: SCR_003070).

2.8. Immunohistochemistry

AXL protein was detected immunohistochemically on formalin fixed paraffin embedded (FFPE) tumor material. The research was conducted only after obtaining the approval of the Bioethics Committee of Maria Sklodowska-Curie National Research Institute of Oncology (Approval no. 73/2018 and 20/2020) and written informed consent was obtained from all participants prior to enrollment. 55 patients were included in a retrospective manner. Immunohistochemical staining was performed on 4-µm FFPE tumor and reference tissue sections using the EnVision FLEX+, Mouse, High pH Detection System (Dako Agilent, no. cat K800221-2). Sections were deparaffinized with xylene and rehydrated in ethanol solutions according to standard procedure. Heat-induced epitope retrieval was carried out in Target Retrieval Solution (Dako Agilent, no. cat S236784-2) for 20 minutes at 98^{o}C. After cooling, the slides were treated for 5 minutes with an endogenous peroxidase blocker (Dako). Slides were incubated with anti-AXL primary monoclonal antibody (C89E7) Rabbit mAb (CST, See Suppl. Data S2.) in 1:100 dilution for 18 hour at 4^{o}C. Slides were subsequently labelled with the Envision Detection System. The color reaction product was developed with 3,3'-diaminobenzidine tetrahydrochloride as a substrate, and nuclear contrast was achieved with hematoxylin counterstaining. The expression of molecular markers was evaluated by a semiquantitative method. Analysis of the results was performed using optical microscopy (magnification ×400). Median expression of protein was determined by Histoscore (H-score) according to formula: $(1\ x\ P_{weak}) + (2\ x\ P_{moderate}) + \left(3\ x\ P_{strong}\right)$, where *P* is the percentage of cells.

2.9. PIV

The retrospective analysis included 55 patients with biopsy-proven metastatic clear cell renal cell carcinoma (mRCC) undergoing cabozantinib treatment as a first line at the Department of Genitourinary Oncology of the Maria Skłodowska-Curie National Research Institute of Oncology in Warsaw (Suppl. Data S2.). Data collection was performed within the framework of the International Consortium for the Analysis of Real-world Outcomes in Renal Cancer (ICARO-RC) project after the Bioethics Committee of Maria Sklodowska-Curie National Research Institute of Oncology approval (Approvals no. 38/2018). All participants were required to provide written informed consent prior to enrollment. The period for data collection was from February 01, 2019 to May 20, 2024. This study was conducted following the principles of the Declaration of Helsinki. Our data set consisted of patient demographics and laboratory test results. The CBC was evaluated before starting the course of treatment. Haematology parameters were measured using Sysmex XN-1000. Laboratory tests were carried out by the Diagnostic Department of National Research Institute of Oncology. PIV was calculated counts of specific cell types with the formula $\frac{NEU\ x\ PLAT\ x\ MON}{LYMPH}$. Counts of inflammatory cells were taken from laboratory results which were done immediately prior to treatment initiation.

2.10. Statistical analysis

Comparison of data between two groups was performed using, two-tailed paired t-test or ordinary one-way ANOVA tests, comparisons involving greater than two groups were performed using a two-way ANOVA analysis of variance test with post hoc Tukey's multiple comparison correction. Results are expressed as mean ± SEM. All statistical tests were estimated using GraphPad Prism (GraphPad software, RRID: SCR_002798). P-values of < 0.05 were considered statistically significant (** $p < 0.05$; ** $p < 0.01$; *** $p < 0.001$; **** $p < 0.0001$*). The illustration was created by web-based BioRender tools (RRID: SCR_018361).

3. Results

3.1. **AXL is present in CD4 + T-cells exhausted by cancer and in TILs in ccRCC patient samples**

In our previous study (Jancewicz et al. Suppl. Table 6), we demonstrated upregulated expression of the AXL gene in exhausted CD4 + T-cells following co-culture with MDA-MB-231 breast cancer cells. A comparable increase in AXL expression was observed in CD4 + T-cells rendered exhausted by renal carcinoma cells (786-O). Furthermore, Western blot analysis confirmed that AXL protein expression was restricted to exhausted CD4 + T-cells (Fig. 1A).

Immunohistochemical analysis of 161 ccRCC specimens (Table 1) demonstrated AXL expression in both tumor cells and tumor-infiltrating T-cells (TILs) (Fig. 1B). Notably, the frequency of AXL-positive TILs was independent of tumor grade and stage (Fig. 1C–D).

Table 1
Patients characteristics.

Gender	**ccRCC patients**
Male	**n = 161 (%)**
Female	**98 (60.9)**
	63 (39.1)
Tumor grade	16 (9.9)
G1	74 (46)
G2	46 (28.6)
G3	20 (12.4)
G4	5 (3.1)
Unknown	
Tumor stage (pT)	88 (54.6)
T1	15 (9.4)
T2	54 (33.5)
T3	3 (1.9)
T4	1 (0.6)
Tx	

[Table 1. Here]

[Figure 1. Here]

3.2. CD4 + T-cells exhibit no sensitivity to the treatment with cabozantinib

Given that cabozantinib is currently used in the treatment of metastatic ccRCC and that AXL is among its therapeutic targets, we investigated whether exhausted CD4 + T-cells are sensitive to cabozantinib treatment. In the study, activated CD4 + T-cells derived from healthy donors were cultured with or without the 786-O ccRCC cancer cell line, with dimethyl sulfoxide (DMSO) or cabozantinib (Fig. 2A). Following a 72-hour incubation period, the cells were collected for subsequent analysis. A marked decrease in the number of CD4 + T-cells was observed in co-culture group (TNT) in comparison to the CD4 + T-cells alone (T15 control). The alterations in CD4 + T-cell proliferation subsequent to drug administration were not observed in either group (T15 DMSO vs. T15 CABO; TNT DMSO vs. TNT CABO) (Fig. 2B). These findings

imply a mutual growth inhibition of CD4 + T-cells and cancer cells in mixed cultures, with cabozantinib exhibiting no discernible effect on this dynamic.

[Figure 2. Here]

3.3. Cabozantinib modulates the expression of key T-cell exhaustion markers

To investigate the molecular landscape of tumor-induced T-cell dysfunction, we profiled the expression of key immunoregulatory molecules in human CD4 + T-cells. CD4 + T-cells from healthy donors were activated and expanded for 12 days, then restimulated and cultured for a further 72 hours either alone (T15) or in co-culture with 786-O renal carcinoma cells (TNT), in the presence of control (DMSO) or cabozantinib. We tested the expression of particular markers both on mRNA and protein levels, namely on the PD-1/PD-L1 exhaustion pathway, as we previously discovered PD-L1 overexpression on exhausted CD4 + T-cells. We analyzed the expression of exhaustion-related molecules at the transcriptional, translational, and surface levels in CD4 + T-cells following co-culture with 786-O tumor cells.

qRT-PCR revealed a consistent pattern of regulation across major immune checkpoint molecules. Cabozantinib treatment significantly downregulated the mRNA expression of the inhibitory receptor PD-1 (CD279) and its ligands, PD-L1 (CD274) and PD-L2 (CD273), in TNT CABO compared to TNT DMSO (Fig. 3A). This transcriptional downregulation was supported at the protein level by Western blot analysis. We observed a congruent trend toward reduced protein expression of PD-1, and PD-L1, in TNT CABO compared to TNT DMSO (Fig. 3B).

Consistent reductions in PD-L1 were detected at the transcript and total protein level, whereas surface expression assessed in flow cytometry remained unchanged or elevated after cabozantinib treatment (Fig. 3C-E) (See Suppl. Data S1. for Gating strategy). This discrepancy suggests that cabozantinib may suppress PD-L1 synthesis while altering its membrane distribution, pointing to complex regulation of checkpoint availability. Collectively, these data indicate that cabozantinib exerts immunomodulatory effects on tumor-conditioned CD4 + T-cells, reshaping exhaustion-associated pathways at both transcriptional and protein levels.

[Figure 3. Here]

Furthermore we analyzed the AXL expression in exhausted CD4 + T-cells treated with cabozantinib. The analysis revealed a profound induction of *AXL* mRNA in CD4 + T-cells co-cultured with 786-O ccRCC cell line (TNT group). The transcript level of *AXL* was elevated over 200-fold in tumor-exposed CD4 + T-cells (TNT DMSO) compared to their tumor-naïve counterparts (T15 DMSO) (Fig. 4A). This transcriptional upregulation was significantly abrogated by treatment with the multi-kinase inhibitor cabozantinib (TNT CABO), which strongly reduced *AXL* expression, suggesting a pharmacologically targetable pathway governs its induction.

Consistent with the transcriptional data, Western blot confirmed a substantial increase in AXL protein expression in TNT DMSO relative to T15 DMSO (Fig. 4B). The full-length isoform 1 (~ 138 kDa) was the predominant form induced and was observed only in TNT groups. Interestingly, although cabozantinib strongly reduced AXL mRNA in exhausted CD4 + T-cells (Fig. 4A), the level of full-length AXL (~ 138 kDa, isoform 1) protein even increased within the 72 h treatment window. In contrast, a lower band of ~ 70 kDa, likely representing either the shorter isoform 3 or a proteolytic fragment of isoform 1, was clearly reduced. Both explanations are consistent with our data: if this band reflects isoform 3, its reduction matches the decrease observed at the transcript level, while if it represents a proteolysis product of isoform 1, the finding is also in line with the Western blot showing stabilization and accumulation of full-length AXL after cabozantinib treatment. Moreover, cabozantinib inhibits AXL activity, but can induce a compensatory feedback loop increasing total AXL expression. This pattern suggests that cabozantinib treatment shifts the AXL protein isoforms towards the mature, full-length form, possibly because it inhibits receptor turnover or alters cleavage, which may be part of the cellular response to kinase inhibition.

[Figure 4. Here]

3.4. Treatment with cabozantinib affects pro-inflammatory and immunosuppressive factors

The persistent presence of pro-inflammatory cytokines IL-1β and IL-6 in TME has been associated with resistance to conventional therapy and immunotherapies [19,20]. Consequently, the modulation of these cytokines is regarded as a promising therapeutic strategy for disrupting tumor-promoting inflammatory cascades. The present study demonstrated that the TNT DMSO group exhibited elevated levels of IL-1β and IL-6 cytokines in comparison with the T15 DMSO group. Conversely, the TNT CABO group demonstrated reduced expression of these cytokines at both the mRNA and protein levels following cabozantinib treatment (see Fig. 5A and 5B) compare to T15 DMSO group. A parallel phenomenon has been identified in the context of cytokines released into the extracellular space (Fig. 5C). The data suggest that cabozantinib may influence the expression/secretion of pro-inflammatory cytokines and has an immunomodulatory effect. Furthermore, as indicated by numerous sources, IL-1β is a component of inflammasome signaling [21], and it has been demonstrated to regulate IL-6 production [22]. It was hypothesized that downregulated IL-1β expression, a result of cabozantinib, could possibly hinder the function of the inflammasome complex as a whole. We performed qRT-PCR of *IL-18* (an inflammasome downstream cytokine) and *NLPR3* (sensor molecule) genes to analyze their mRNA expression in each treated CD4 + T-cell group. A significant increase in IL-18 relative transcript level was observed; however, NLPR3 expression was found to be strongly elevated following cabozantinib treatment (Fig. 5D). The findings indicate that, inflammasome is not overall affected but its activity can be impaired, thereby modulating IL-1βlevels. Another explanation is, that IL-1β transcript is strongly downregulated (more than 10 times), therefore the IL-1β cytokine level is highly reduced.

Concurrently, in group TNT CABO we observed significantly higher expression of immunosuppressive molecules, such as TGFβ2 and IDO1 after cabozantinib treatment (Fig. 5E and 5F). This cytokine may contribute to a “rebalancing” effect, whereby cabozantinib suppresses acute pro-inflammatory mediators (IL-1β, IL-6), thereby reducing inflammation within the tumor microenvironment (TME), while concurrently increasing TGFβ2 and IDO1 expression to promote immunosuppression and shift the response toward a tolerogenic state. It is important to note that this shift can promote immune escape if IDO1 dominates [23]. These effects are often amplified in hypoxic or MET/AXL-high environments, supporting cabozantinib role in combination immunotherapies.

[Figure 5. Here]

3.5. Cabozantinib modifies extracellular cytokine profile of CD4 + T-cells in the presence of tumor cells

Significant changes in pro-inflammatory cytokine levels prompted us to characterize the cytokine profile of the CD4 + T-cell environment before and after treatment with cabozantinib in the presence of renal cancer tumor cells. The cytokine array (See Suppl. Data S1. for whole Cytokine Array figures) demonstrated a substantial decrease in the expression levels of IL-2, IFN-y, TNF-a, and G-CSF in the TNT CABO group compared to the TNT DMSO group. Concurrently, an escalation in the secretion of GM-CSF was observed (Fig. 6A, 6B and 6C). The results of the study indicate that after cabozantinib treatment exhausted CD4 + T-cells may exhibit diminished capacity to trigger pro-inflammatory or cytotoxic responses [24], simultaneously reducing tumor-promoting inflammation [16].

[Figure 6. Here]

3.6. Cabozantinib reduces inflammatory markers observed in complete blood counts

Complete blood count (CBC) results showed a significant reduction in neutrophil, platelet and monocyte levels between baseline and week 12 of cabozantinib treatment (Fig. 7-D-E). Similarly, composite inflammatory indices, including the pan-immune-inflammation value (PIV) and PIV divided by Hb, were statistically decreased (p-value = 0.031 and 0.0124 respectively) (Fig. 7A and 7B). Interestingly, the level of lymphocytes was only slightly changed after 12 weeks of cabozantinib treatment, with tendency of higher count (Fig. 7C). These findings are consistent with reduced systemic inflammatory indices during treatment, although treatment-related hematologic effects cannot be excluded. Potentially, this relationship may be related to the reduction in pro-inflammatory cytokines observed in vitro. It is also possible that the observed correlation results from bone marrow suppression, but it should be noted that hemoglobin levels increase after treatment, as can be seen in PIV/Hb. The average changes for monocyte, platelet, and neutrophil levels were 28.5%, 25.6%, and 23%, respectively. We also observed an average increase in lymphocyte count and hemoglobin level of 6.2% and 6.5%, respectively, but it was not statistically significant. Changes in PIV and PIV/Hb were 63.8% and 70.1%, respectively.

[Figure 7. Here]

4. Discussion

The treatment of advanced renal cell carcinoma (aRCC) has been revolutionized by the advent of VEGFR-TKIs and subsequently ICIs. Cabozantinib has demonstrated significant clinical activity in aRCC, both as a monotherapy and in combination with ICIs [25–27]. The rationale for combining TKIs with ICIs stems from the potential for synergistic effects, where TKIs may modulate the TME to be more permissive to an anti-tumor immune response [25]. The study aimed to elucidate the immunomodulatory effects of cabozantinib on CD4 + T-cells, a critical component of the anti-tumor immune response whose role in the context of TKI therapy is not fully understood. The findings reveal that cabozantinib can modulate an interplay between CD4 + T-cells infiltrating tumor, and tumor cells, providing novel insights into the mechanisms underlying the clinical efficacy of this treatment.

The mutual growth inhibition observed between CD4 + T-cells and cancer cells in co-culture represents a fundamental aspect of tumor-immune system interactions that has been extensively documented in the literature, including our previous studies [6,28–30]. Our data indicate that cabozantinib did not directly impact the proliferation of activated CD4 + T-cells in our co-culture system. The absence of direct cabozantinib influence on T-cell activity may support further evaluation of combination strategies, but does not by itself predict clinical safety. [11,16,31,32]. By inhibiting VEGFR, TKIs seal leaky blood vessels within the tumor and reduce tissue pressure, which enhances T-cell infiltration [16,33,34]. Moreover, some studies indicate that cabozantinib could enhance T-cell infiltration through a second, independent mechanism. In breast cancer models, AXL knockout significantly increased both CD4 + and CD8 + T-cell numbers, with fold increases in CD8 + T-cell proportions ranging from 4.9 to 40.7-fold depending on treatment conditions. Similarly, AXL inhibition in head and neck cancer led to enhanced infiltration of cytotoxic immune cells including CD8 + T-cells and NK cells, while reducing immunosuppressive cell populations [35,36].

High AXL expression is frequently associated with poor prognoses in various cancer types, partially due to its role in immune modulation and creation of immunosuppressive conditions within TME, consequently inducing a state of T-cell exhaustion [37]. Our data reveal that AXL is a highly inducible factor which increases during CD4 + T-cells exhaustion derived by tumor, consistently with broader evidence linking AXL to tumor progression across cancer types and cellular contexts [38,39]. Furthermore, AXL expression is associated with reduced release of pro-inflammatory cytokines, suppression of TLR-mediated inflammatory signaling, and decreased antigen presentation through MHC-I [35,40,41]. Preclinical evidence indicates that AXL appears to be a key checkpoint in dendritic cells, where its loss amplifies type I interferon activity, in turn inhibiting IL-1β production and disrupting dendritic cell maturation [42,43]. This finding complements our observation of AXL induction in tumor-conditioned CD4 + T-cells, suggesting that AXL may constitute a coordinated immunosuppressive checkpoint.

Furthermore, AXL overexpression was demonstrated as early as two decades ago in the context of kidney cancers, and subsequently in inflammatory kidney diseases [44,45]. Hypoxia-inducible factors HIF-1 and HIF-2 have been shown to directly regulate the AXL promoter, suggesting that microenvironmental hypoxia may contribute to the profound induction observed in our tumor co-culture system [46]. Further studies have shown that AXL may also be a prognostic factor in renal tumors, as the group with lower AXL expression showed longer survival [47]. AXL also contributes to resistance to immuno-oncology therapies by driving macrophage polarization towards an immunosuppressive, pro-tumor M2-like phenotype [48,49]. This proceeds largely via efferocytosis of apoptotic cells. By inhibiting AXL, we interrupt the Gas6–AXL/MerTK axis that sustains M2-like polarization, breaking the efferocytosis-driven positive loop and dampening PI3K–Akt with downstream NF-κB/STAT signaling that favors M2 traits. In our dataset, cabozantinib was associated with reduced IL-4 and IL-10 – cytokines that reinforce M2 macrophages via STAT6/STAT3, thereby weakening M2-skewing cues and facilitating repolarization toward an M1-like state [50,51]. As demonstrated by the analyses from the COSMIC-313 study, it appears that cabozantinib overcomes immunosuppression and restores the activity of immunotherapy, particularly in patients with high levels of M2 macrophages [52]. Moreover, data from the clinical part of this study demonstrated that after 12 weeks of cabozantinib treatment, level of monocytes decreases by 28,5%. The number of monocytes constitutes the sole indirect indicator of the potential number of macrophages present within the tissue following differentiation.

Additionally, AXL expression has been positively correlated with PD-L1 levels in RCC, suggesting a link between AXL signaling and immune evasion and resistance to immune checkpoint inhibitors [53]. These external data are in line with our observation that cabozantinib can modulate PD-1/PD-L1 pathway components, supporting the view that AXL may act as part of an exhaustion program in tumor-exposed CD4 + T-cells [53,54]. Such dual action may underlie the reported clinical synergy between cabozantinib and immune checkpoint inhibitors in RCC and other malignancies [25,31,33]. The complexity of PD-L1 regulation at transcript, protein, and surface levels further underscores the need for integrative functional studies to define how modulation of checkpoint pathways by cabozantinib translates into restored effector capacity. Collectively, these observations suggest that AXL contributes to CD4 + T-cell dysfunction in the tumor context, while cabozantinib, by attenuating both AXL and canonical inhibitory pathways, may help create a more favorable immune environment for checkpoint-based therapies.

The Gas6/Axl signaling pathway has been demonstrated to promote the secretion of immunosuppressive chemokines, including CCL3-5, G-CSF, IL-3, IL-4, IL-6, IL-12_p70, TGFβ, and TNFα. This cytokine profile fosters an unfavorable environment for anti-tumor immune responses [55]. A variety of studies have underscored the immunomodulatory effects of cabozantinib, which are associated with its AXL-targeting functionality. The beneficial collaboration between drugs seems to boost immunosurveillance mechanisms mainly through simultaneous PD-1 blockade and inhibition by cabozantinib of Tyro3/AXL/MER (TAM) receptors. This results in an inhibitory effect on immunosuppressor factors, such as IL-10, IL-6, GAS6, ARG1, EZH2 or HIF1A; and activation of immunostimulatory molecules, including IFNG and IL2 [34]. Our investigation into the cytokine profile of

the co-cultures revealed that cabozantinib exerts a dual effect on the TME. It significantly reduced the levels of the pro-inflammatory cytokines IL-1β and IL-6. This is a crucial finding, as chronic inflammation driven by these cytokines is known to promote tumor growth, angiogenesis, and immunosuppression [56,57]. Furthermore, IL-1β increases granulocyte–macrophage colony-forming units (CFU-GM) in the bone marrow, thereby enhancing the production of neutrophils [58,59]. It also accelerates neutrophil mobilization by promoting the release of both mature and immature forms from marrow reserves, while IL-6 further drives their egress into the circulation and depletes marrow stores [60]. In addition, IL-1β prolongs neutrophil survival by delaying apoptosis in the presence of mononuclear cells through inflammasome-dependent mechanisms [61]. Notably, platelets function as both targets and sources of IL-1β: despite being anucleate, they can synthesize and release this cytokine via distinctive post-transcriptional splicing and translational processes [62]. Complementing these effects, IL-6 induces hepatic thrombopoietin (TPO) transcription and drives thrombopoiesis, producing the reactive thrombocytosis typical of inflammatory states [63,64]. As we have shown, cabozantinib is associated with a 25,6% decrease in circulating platelets and a 23% decrease in neutrophils. These clinical observations are consistent with our findings in a co-culture model and suggest that the observed immunoinflammatory shifts may extend to the whole organism. By dampening tumor-associated inflammation – and thereby curbing pro-inflammatory cytokine release – cabozantinib may contribute to lower peripheral neutrophil and platelet counts through reduced inflammatory signaling, although the underlying mechanism remains unresolved.

The reduction in IL-1β and IL-6 levels, concomitant with the paradoxical elevation of *NLRP3* gene expression, suggests that cabozantinib may disrupt inflammasome activity through post-translational mechanisms while preserving the cellular machinery for future inflammatory responses [65,66]. The concurrent elevation of immunosuppressive mediators TGFβ2 and IDO1 represents a compensatory mechanism that may serve both beneficial and detrimental functions in the therapeutic context. Although increased IDO1 expression traditionally correlates with immune suppression and therapy resistance through tryptophan depletion and kynurenine pathway activation, recent evidence suggests that this upregulation may represent a transient adaptive response that prevents excessive immune activation [67]. The elevated expression of TGFβ2, as opposed to TGFβ1, signifies the activation of discrete signaling pathways that may facilitate tissue regeneration and vascular remodeling, rather than merely immunosuppression. This interpretation is supported by the discoveries demonstrating that TGFβ2 can drive type 2 immunity responses that promote vascular reorganization and cancer cell containment through hypoxia-induced death mechanisms [68]. This cytokine profile represents a "rebalancing" where cabozantinib suppresses acute pro-inflammatory drivers (IL-1β, IL-6) to reduce TME immunosuppression. Concurrently, the drug elevates TGFβ2 and IDO1, aiming to promote tolerogenic responses. In CD4 + T-cell-tumor co-cultures, this shift has the potential to enhance anti-tumor efficacy by improving CD4 + T-cell infiltration and function. However, it is important to note that this shift can also promote immune escape if IDO1 dominates. These effects are context-dependent, often amplified in hypoxic or MET/AXL-high environments, supporting the role of cabozantinib in combination with immunotherapies [69,70].

On the other hand, further characterization of the cytokine milieu in the co-culture supernatants revealed a significant decrease in the secretion of key effector cytokines IL-2, IFN-γ, and TNF-α by CD4 + T-cells after cabozantinib treatment. This reduction in effector cytokines is a hallmark of T-cell exhaustion [71,72]. However, in the context of cabozantinib treatment, this might not be solely a negative outcome. By dampening the chronic inflammatory signaling in the TME, cabozantinib could be preventing further CD4 + T-cell exhaustion and creating a more favorable environment for a sustained anti-tumor response. IL-2, IFN-γ, and TNF-α are hallmark Th1 cytokines involved in T-cell proliferation (IL-2), cytotoxicity, and classical anti-tumor immune responses (IFN-γ, TNF-α). Cabozantinib, by inhibition of key tyrosine kinase pathways, compromises signals essential for robust Th1-type responses, especially in a suppressive tumor microenvironment. The resulting decreased expression of these cytokines suggests that exhausted or alternatively-polarized CD4 + T-cells can be less able to mount pro-inflammatory or cytotoxic responses following cabozantinib treatment [16,24].

Cabozantinib reduced G-CSF secretion while increasing GM-CSF levels, indicating a broader remodeling of the extracellular cytokine milieu in tumor-conditioned CD4 T cells. Together with the reduced IL-1 and IL-6 expression observed in this model, these changes are consistent with attenuation of inflammatory signaling, although the functional consequences of increased GM-CSF in the TME remain context-dependent [73].

The comprehensive dataset presented in this study reveals cabozantinib as a multifaceted immunomodulator that acts through several interconnected mechanisms. The dramatic induction of AXL in tumor exhausted CD4 + T-cells, along with its subsequent modulation by cabozantinib support a model in which cabozantinib reshapes inflammatory and exhaustion-associated programs in tumor-conditioned CD4 T cells. The observation of complex cytokine remodeling indicates that cabozantinib does not merely reverse tumor-induced changes, but rather establishes a distinctly different immune environment with strong reduction of master pro-inflammatory cytokines (IL-1β and IL-6). The clinical relevance of these findings is supported by the growing body of evidence for cabozantinib plus immunotherapy combinations across multiple cancer types. However, the complex nature of the immune remodeling observed suggests that optimal combination strategies may require careful timing and patient selection. The heterogeneous AXL expression patterns observed in patient samples underscore the necessity for biomarker-driven approaches to maximize therapeutic benefit.

Declarations

Conflict of interest:

The authors declare that the research was conducted in the absence of any commercial or financial relationships that could be construed as potential conflicts of interest.

Ethic statement

All procedures in this study were conducted in accordance with the Bioethics Committee of Maria Sklodowska-Curie National Research Institute of Oncology (Approvals no. 73/2018, 38/2018 and 20/2020).

Framework

The retrospective studies involved patients treated between 2019 and 2024, while the *in vitro* studies were conducted between 2023 and 2025.

Author Contribution

Conceptualization: ES, JK, PD, MS; data curation: ES, SM; formal analysis: ES, MS, PD, PW, SM, MŁ; funding acquisition: PD; investigation: PD, MS, NR, AŚ; methodology: ES, SM; project administration: ES, JK, PW; resources: JK, PW, MŁ, ES; supervision: ES, SM; validation: ES, SM; visualization: MS; writing-original draft: MS, PD; writing-review and editing: ES, NR, AŚ, JK, PW, SM, MŁ. All the authors have read and agreed to the published version of the manuscript.

Acknowledgement

We would like to express our profound gratitude to the MSNCRIO Department of Genitourinary Oncology for support and paraffin-embedded sample preparation. This study was supported by the MSCNRIO Intramural Research Program (SN/MGW8/2025). No external funding was received for this work.

Data Availability

Supporting data associated with the main manuscript and supplementary materials are provided in the Supplementary Data S1-S3 files. The data that support the findings of this study are available from the corresponding author, ES, upon reasonable request.

References

1. Capitanio, U. et al. Epidemiology of Renal Cell Carcinoma. *Eur. Urol.* **75**, 74–84. https://doi.org/10.1016/j.eururo.2018.08.036 (2019).
2. Padala, S. A. et al. Epidemiology of Renal Cell Carcinoma. *World J. Oncol.* **11**, 79–87. https://doi.org/10.14740/wjon1279 (2020).
3. Linehan, W. M. Genetic basis of kidney cancer: role of genomics for the development of disease-based therapeutics. *Genome Res.* **22**, 2089–2100. https://doi.org/10.1101/gr.131110.111 (2012).
4. Şenbabaoğlu, Y. et al. Tumor immune microenvironment characterization in clear cell renal cell carcinoma identifies prognostic and immunotherapeutically relevant messenger RNA signatures.

Genome Biol. **17**, 231. https://doi.org/10.1186/s13059-016-1092-z (2016).

5. Escors, D. et al. Systemic CD4 Immunity and PD-L1/PD-1 Blockade Immunotherapy. *Int. J. Mol. Sci.* **23** https://doi.org/10.3390/ijms232113241 (2022).
6. Jancewicz, I. et al. PD-L1 Overexpression, SWI/SNF Complex Deregulation, and Profound Transcriptomic Changes Characterize Cancer-Dependent Exhaustion of Persistently Activated CD4(+) T Cells. *Cancers (Basel)*. 13. https://doi.org/10.3390/cancers13164148 (2021).
7. Shedlock, D. J. & Shen, H. Requirement for CD4 T cell help in generating functional CD8 T cell memory. *Science* **300**, 337–339. https://doi.org/10.1126/science.1082305 (2003).
8. Ahrends, T. et al. CD4(+) T cell help creates memory CD8(+) T cells with innate and help-independent recall capacities. *Nat. Commun.* **10**, 5531. https://doi.org/10.1038/s41467-019-13438-1 (2019).
9. Quezada, S. A. et al. Tumor-reactive CD4(+) T cells develop cytotoxic activity and eradicate large established melanoma after transfer into lymphopenic hosts. *J. Exp. Med.* **207**, 637–650. https://doi.org/10.1084/jem.20091918 (2010).
10. Perez-Diez, A. et al. CD4 cells can be more efficient at tumor rejection than CD8 cells. *Blood* **109**, 5346–5354. https://doi.org/10.1182/blood-2006-10-051318 (2007).
11. Choueiri, T. K. et al. Cabozantinib plus Nivolumab and Ipilimumab in Renal-Cell Carcinoma. *N. Engl. J. Med.* **388**, 1767–1778. https://doi.org/doi:10.1056/NEJMoa2212851 (2023).
12. Motzer, R. J. et al. Sunitinib versus interferon alfa in metastatic renal-cell carcinoma. *N Engl. J. Med.* **356**, 115–124. https://doi.org/10.1056/NEJMoa065044 (2007).
13. Ott, P. A., Hodi, F. S. & Buchbinder, E. I. Inhibition of Immune Checkpoints and Vascular Endothelial Growth Factor as Combination Therapy for Metastatic Melanoma: An Overview of Rationale, Preclinical Evidence, and Initial Clinical Data. *Front. Oncol.* **5**, 202. https://doi.org/10.3389/fonc.2015.00202 (2015).
14. Voron, T. et al. Control of the immune response by pro-angiogenic factors. *Front. Oncol.* **4**, 70. https://doi.org/10.3389/fonc.2014.00070 (2014).
15. Apolo, A. B. et al. Cabozantinib in patients with platinum-refractory metastatic urothelial carcinoma: an open-label, single-centre, phase 2 trial. *Lancet Oncol.* **21**, 1099–1109. https://doi.org/10.1016/s1470-2045(20)30202-3 (2020).
16. Kwilas, A. R., Ardiani, A., Donahue, R. N., Aftab, D. T. & Hodge, J. W. Dual effects of a targeted small-molecule inhibitor (cabozantinib) on immune-mediated killing of tumor cells and immune tumor microenvironment permissiveness when combined with a cancer vaccine. *J. Translational Med.* **12** https://doi.org/10.1186/s12967-014-0294-y (2014).
17. Ladner, C. L., Yang, J., Turner, R. J. & Edwards, R. A. Visible fluorescent detection of proteins in polyacrylamide gels without staining. *Anal. Biochem.* **326**, 13–20. https://doi.org/10.1016/j.ab.2003.10.047 (2004).
18. Rao, X., Huang, X., Zhou, Z. & Lin, X. An improvement of the 2ˆ(-delta delta CT) method for quantitative real-time polymerase chain reaction data analysis. *Biostat Bioinforma Biomath*. **3**, 71–85 (2013).

19. Beyranvand Nejad, E. et al. Interleukin-6-mediated resistance to immunotherapy is linked to impaired myeloid cell function. *Int. J. Cancer*. **148**, 211–225. https://doi.org/10.1002/ijc.33280 (2021).
20. Kiss, M. et al. IL1β Promotes Immune Suppression in the Tumor Microenvironment Independent of the Inflammasome and Gasdermin D. *Cancer Immunol. Res.* **9**, 309–323. https://doi.org/10.1158/2326-6066.Cir-20-0431 (2021).
21. Zheng, D., Liwinski, T. & Elinav, E. Inflammasome activation and regulation: toward a better understanding of complex mechanisms. *Cell. Discov*. **6**, 36. https://doi.org/10.1038/s41421-020-0167-x (2020).
22. Munoz, L., Yeung, Y. T. & Grewal, T. Oncogenic Ras modulates p38 MAPK-mediated inflammatory cytokine production in glioblastoma cells. *Cancer Biol. Ther.* **17**, 355–363. https://doi.org/10.1080/15384047.2016.1139249 (2016).
23. Bishnupuri, K. S. et al. IDO1 and Kynurenine Pathway Metabolites Activate PI3K-Akt Signaling in the Neoplastic Colon Epithelium to Promote Cancer Cell Proliferation and Inhibit Apoptosis. *Cancer Res.* **79**, 1138–1150. https://doi.org/10.1158/0008-5472.Can-18-0668 (2019).
24. Lu, C. et al. Understanding the dynamics of TKI-induced changes in the tumor immune microenvironment for improved therapeutic effect. *J. Immunother Cancer*. **12** https://doi.org/10.1136/jitc-2024-009165 (2024).
25. Choueiri, T. K. et al. Nivolumab plus Cabozantinib versus Sunitinib for Advanced Renal-Cell Carcinoma. *N. Engl. J. Med.* **384**, 829–841. https://doi.org/10.1056/nejmoa2026982 (2021).
26. Choueiri, T. K. et al. Cabozantinib Versus Sunitinib As Initial Targeted Therapy for Patients With Metastatic Renal Cell Carcinoma of Poor or Intermediate Risk: The Alliance A031203 CABOSUN Trial. *J. Clin. Oncol.* **35**, 591–597. https://doi.org/10.1200/jco.2016.70.7398 (2017).
27. Choueiri, T. K.et al. Cabozantinib versus everolimus in advanced renal cell carcinoma (METEOR): final results from a randomised, open-label, phase 3 trial. *Lancet Oncol* 17, 917–927 (2016). https://doi.org/10.1016/S1470-2045(16)30107-3.
28. Stachowiak, M. et al. Cancer cells accelerate exhaustion of persistently activated mouse CD4(+) T cells. *Oncoimmunology* **14**, 2521392. https://doi.org/10.1080/2162402x.2025.2521392 (2025).
29. Lowther, D. E. et al. PD-1 marks dysfunctional regulatory T cells in malignant gliomas. *JCI Insight*. **1** https://doi.org/10.1172/jci.insight.85935 (2016).
30. Nakano, M. et al. PD-1 + TIM-3 + T cells in malignant ascites predict prognosis of gastrointestinal cancer. *Cancer Sci.* **109**, 2986–2992. https://doi.org/10.1111/cas.13723 (2018).
31. Su, J. et al. Cabozantinib in combination with immune checkpoint inhibitors for renal cell carcinoma: a systematic review and meta-analysis. *Front. Pharmacol.* **15**, 1322473. https://doi.org/10.3389/fphar.2024.1322473 (2024).
32. Krawczyk, K., Śladowska, K., Holko, P. & Kawalec, P. Comparative safety of tyrosine kinase inhibitors in the treatment of metastatic renal cell carcinoma: a systematic review and network meta-analysis. *Front. Pharmacol.* **14**, 1223929. https://doi.org/10.3389/fphar.2023.1223929 (2023).

33. Esteban-Fabró, R. et al. Cabozantinib Enhances Anti-PD1 Activity and Elicits a Neutrophil-Based Immune Response in Hepatocellular Carcinoma. *Clin. Cancer Res.* **28**, 2449–2460. https://doi.org/10.1158/1078-0432.Ccr-21-2517 (2022).
34. Durán, I. et al. Exploring the synergistic effects of cabozantinib and a programmed cell death protein 1 inhibitor in metastatic renal cell carcinoma with machine learning. *Oncotarget* **13**, 237–256. https://doi.org/10.18632/oncotarget.28183 (2022).
35. Aguilera, T. A. & Giaccia, A. J. Molecular Pathways: Oncologic Pathways and Their Role in T-cell Exclusion and Immune Evasion-A New Role for the AXL Receptor Tyrosine Kinase. *Clin. Cancer Res.* **23**, 2928–2933. https://doi.org/10.1158/1078-0432.Ccr-17-0189 (2017).
36. Aguilera, T. A. et al. Reprogramming the immunological microenvironment through radiation and targeting Axl. *Nat. Commun.* **7**, 13898. https://doi.org/10.1038/ncomms13898 (2016).
37. Guo, Z., Li, Y., Zhang, D. & Ma, J. Axl inhibition induces the antitumor immune response which can be further potentiated by PD-1 blockade in the mouse cancer models. *Oncotarget* **8**, 89761–89774. https://doi.org/10.18632/oncotarget.21125 (2017).
38. Zhou, L. et al. Targeting MET and AXL Overcomes Resistance to Sunitinib Therapy in Renal Cell Carcinoma. *Oncogene* **35**, 2687–2697. https://doi.org/10.1038/onc.2015.343 (2015).
39. Mikami, S. et al. Increased Expression of AXL and C-MET in High-Grade Clear Cell Renal Cell Carcinoma and Its Association With VEGFR-TKI Treatment and PD-L1 Expression. *Pathology International* (2025). https://doi.org/10.1111/pin.70030
40. Gay, C. M., Balaji, K. & Byers, L. A. Giving AXL the axe: targeting AXL in human malignancy. *Br. J. Cancer*. **116**, 415–423. https://doi.org/10.1038/bjc.2016.428 (2017).
41. Zhu, C., Wei, Y. & Wei, X. AXL receptor tyrosine kinase as a promising anti-cancer approach: functions, molecular mechanisms and clinical applications. *Mol. Cancer*. **18**, 153. https://doi.org/10.1186/s12943-019-1090-3 (2019).
42. Schmid, E. T. et al. AXL receptor tyrosine kinase is required for T cell priming and antiviral immunity. *Elife* **5** https://doi.org/10.7554/eLife.12414 (2016).
43. Aguilera, T. et al. Axl inhibition on dendritic cells enhances STING anticancer therapy through type I interferon signaling. (2024).
44. Fiebeler, A. et al. Growth arrest specific protein 6/Axl signaling in human inflammatory renal diseases. *Am. J. Kidney Dis.* **43**, 286–295. https://doi.org/10.1053/j.ajkd.2003.10.016 (2004).
45. Chung, B. I., Malkowicz, S. B., Nguyen, T. B., Libertino, J. A. & McGarvey, T. W. Expression of the proto-oncogene Axl in renal cell carcinoma. *DNA Cell. Biol.* **22**, 533–540. https://doi.org/10.1089/10445490360708946 (2003).
46. Rankin, E. B. et al. Direct regulation of GAS6/AXL signaling by HIF promotes renal metastasis through SRC and MET. *Proceedings of the National Academy of Sciences* 111, 13373–13378 (2014). https://doi.org/10.1073/pnas.1404848111
47. Gustafsson, A. et al. Differential expression of Axl and Gas6 in renal cell carcinoma reflecting tumor advancement and survival. *Clin. Cancer Res.* **15**, 4742–4749. https://doi.org/10.1158/1078-

0432.Ccr-08-2514 (2009).

48. Engelsen, A. S. T. et al. Dissecting the Role of AXL in Cancer Immune Escape and Resistance to Immune Checkpoint Inhibition. *Front. Immunol.* **13**, 869676. https://doi.org/10.3389/fimmu.2022.869676 (2022).
49. Aehnlich, P., Powell, R. M., Peeters, M. J. W. & Rahbech, A. Thor Straten, P. TAM Receptor Inhibition-Implications for Cancer and the Immune System. *Cancers (Basel)*. 13. https://doi.org/10.3390/cancers13061195 (2021).
50. Wu, G. et al. Targeting Gas6/TAM in cancer cells and tumor microenvironment. *Mol. Cancer*. **17**, 20. https://doi.org/10.1186/s12943-018-0769-1 (2018).
51. Myers, K. V., Amend, S. R. & Pienta, K. J. Targeting Tyro3, Axl and MerTK (TAM receptors): implications for macrophages in the tumor microenvironment. *Mol. Cancer*. **18**, 94. https://doi.org/10.1186/s12943-019-1022-2 (2019).
52. Laurence Albiges, R. M. et al. Emilio Esteban, Jose Angel Arranz Arija, Scott Tykodi, Haijun Ma, Lei Zhou, Maximiliano Van Kooten Losio, Andrew Simmons, Fatima Rangwala, Cabozantinib (C) in combination with nivolumab (N) and ipilimumab (I) in previously untreated advanced renal cell carcinoma (aRCC): Final results of COSMIC-313., (J Clin Oncol 43, (suppl 5; abstr 438)). (2025).
53. Terry, S. et al. Association of AXL and PD-L1 Expression with Clinical Outcomes in Patients with Advanced Renal Cell Carcinoma Treated with PD-1 Blockade. *Clin. Cancer Res.* **27**, 6749–6760. https://doi.org/10.1158/1078-0432.Ccr-21-0972 (2021).
54. Santoni, M. et al. Antitumor Effects of the Multi-Target Tyrosine Kinase Inhibitor Cabozantinib: A Comprehensive Review of the Preclinical Evidence. *Expert Rev. Anticancer Ther.* **21**, 1029–1054. https://doi.org/10.1080/14737140.2021.1919090 (2021).
55. Tanaka, M. & Siemann, D. W. Gas6/Axl Signaling Pathway in the Tumor Immune Microenvironment. *Cancers (Basel)*. 12. https://doi.org/10.3390/cancers12071850 (2020).
56. Bent, R., Moll, L., Grabbe, S. & Bros, M. Interleukin-1 Beta-A Friend or Foe in Malignancies? *Int. J. Mol. Sci.* **19** https://doi.org/10.3390/ijms19082155 (2018).
57. Li, R., Wen, A. & Lin, J. Pro-Inflammatory Cytokines in the Formation of the Pre-Metastatic Niche. *Cancers (Basel)*. 12. https://doi.org/10.3390/cancers12123752 (2020).
58. Flores-Gomez, D. et al. Interleukin-1β induces trained innate immunity in human hematopoietic progenitor cells in vitro. *Stem Cell. Rep.* **19**, 1651–1664. https://doi.org/10.1016/j.stemcr.2024.09.004 (2024).
59. Fibbe, W. E. et al. Interleukin-1 (22-K Factor) Induces Release of Granulocyte-Macrophage Colony-Stimulating Activity From Human Mononuclear Phagocytes. *Blood* **68**, 1316–1321. https://doi.org/https://doi.org/10.1182/blood.V68.6.1316.1316 (1986).
60. Florentin, J. et al. Interleukin-6 mediates neutrophil mobilization from bone marrow in pulmonary hypertension. *Cell. Mol. Immunol.* **18**, 374–384. https://doi.org/10.1038/s41423-020-00608-1 (2021).

61. Christenson, K., Björkman, L., Karlsson, A. & Bylund, J. Regulation of neutrophil apoptosis differs after in vivo transmigration to skin chambers and synovial fluid: a role for inflammasome-dependent interleukin-1β release. *J. Innate Immun.* **5**, 377–388. https://doi.org/10.1159/000350378 (2013).
62. Brown, G. T., Narayanan, P., Li, W., Silverstein, R. L. & McIntyre, T. M. Lipopolysaccharide stimulates platelets through an IL-1β autocrine loop. *J. Immunol.* **191**, 5196–5203. https://doi.org/10.4049/jimmunol.1300354 (2013).
63. Wolber, E. M. & Jelkmann, W. Interleukin-6 increases thrombopoietin production in human hepatoma cells HepG2 and Hep3B. *J. Interferon Cytokine Res.* **20**, 499–506. https://doi.org/10.1089/10799900050023915 (2000).
64. Kaser, A. et al. Interleukin-6 stimulates thrombopoiesis through thrombopoietin: role in inflammatory thrombocytosis. *Blood* **98**, 2720–2725. https://doi.org/10.1182/blood.v98.9.2720 (2001).
65. Tengesdal, I. W. et al. Tumor NLRP3-Derived IL-1β Drives the IL-6/STAT3 Axis Resulting in Sustained MDSC-Mediated Immunosuppression. *Front. Immunol.* **12**, 661323. https://doi.org/10.3389/fimmu.2021.661323 (2021).
66. Guo, B., Fu, S., Zhang, J., Liu, B. & Li, Z. Targeting inflammasome/IL-1 pathways for cancer immunotherapy. *Sci. Rep.* **6**, 36107. https://doi.org/10.1038/srep36107 (2016).
67. Gomes, B. et al. Characterization of the Selective Indoleamine 2,3-Dioxygenase-1 (IDO1) Catalytic Inhibitor EOS200271/PF-06840003 Supports IDO1 as a Critical Resistance Mechanism to PD-(L)1 Blockade Therapy. *Mol. Cancer Ther.* **17**, 2530–2542. https://doi.org/10.1158/1535-7163.Mct-17-1104 (2018).
68. Liu, M. et al. TGF-β suppresses type 2 immunity to cancer. *Nature* **587**, 115–120. https://doi.org/10.1038/s41586-020-2836-1 (2020).
69. Scirocchi, F. et al. Immunogenic Cell Death and Immunomodulatory Effects of Cabozantinib. *Front. Oncol.* **11**, 755433. https://doi.org/10.3389/fonc.2021.755433 (2021).
70. Koinis, F. et al. Resistance to MET/VEGFR2 Inhibition by Cabozantinib Is Mediated by YAP/TBX5-Dependent Induction of FGFR1 in Castration-Resistant Prostate Cancer. *Cancers (Basel)*. 12. https://doi.org/10.3390/cancers12010244 (2020).
71. Miggelbrink, A. M. et al. CD4 T-Cell Exhaustion: Does It Exist and What Are Its Roles in Cancer? *Clin. Cancer Res.* **27**, 5742–5752. https://doi.org/10.1158/1078-0432.Ccr-21-0206 (2021).
72. Accogli, T., Bruchard, M. & Végran, F. Modulation of CD4 T Cell Response According to Tumor Cytokine Microenvironment. *Cancers (Basel)*. 13. https://doi.org/10.3390/cancers13030373 (2021).
73. Kumar, A., Taghi Khani, A., Sanchez Ortiz, A. & Swaminathan, S. GM-CSF: A Double-Edged Sword in Cancer Immunotherapy. *Front. Immunol.* **13**, 901277. https://doi.org/10.3389/fimmu.2022.901277 (2022).

Figures

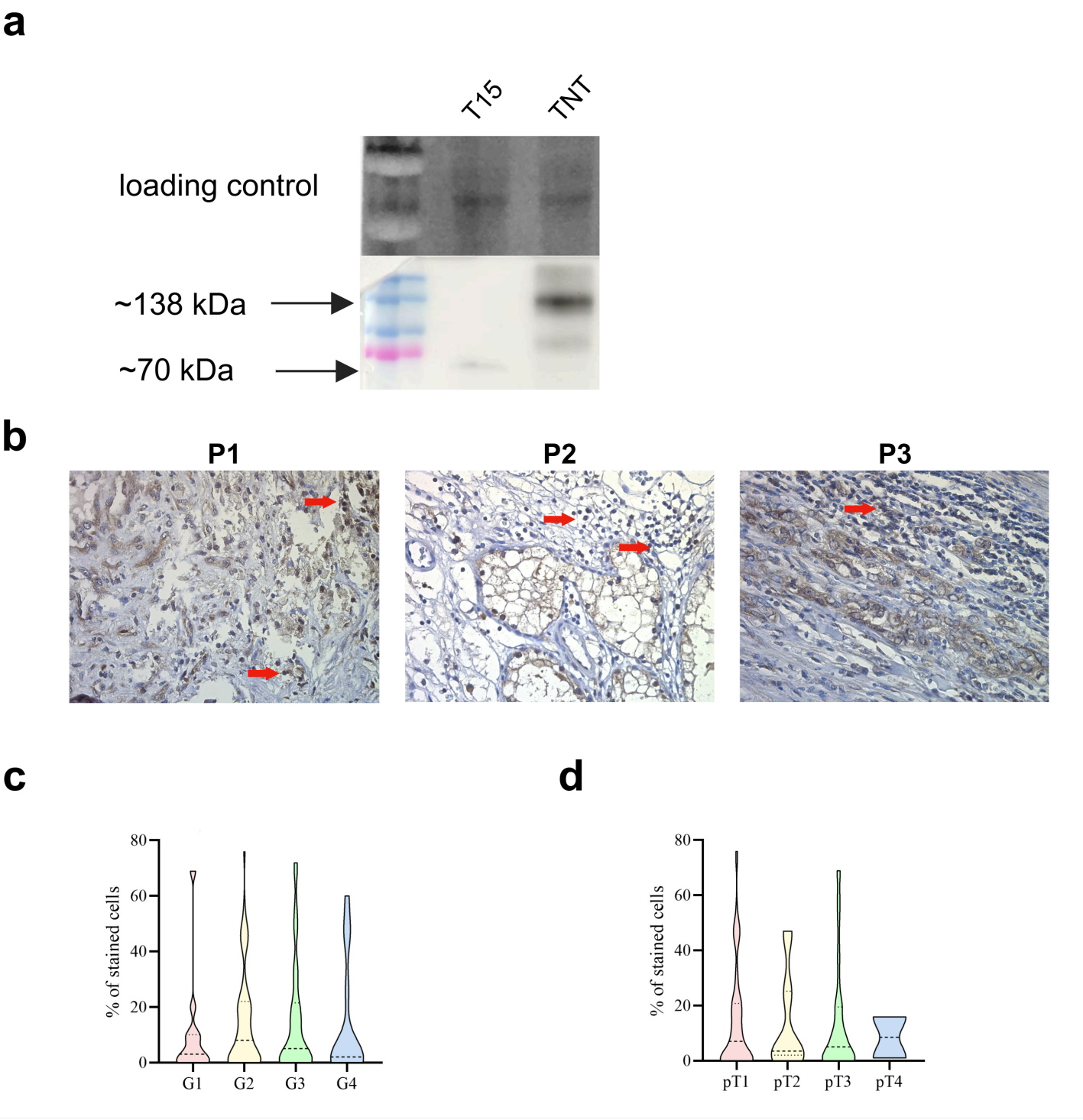


Figure 1

AXL abundance in TILs in ccRCC patient samples. (a) AXL protein expression level identified in control and exhausted CD4+ T-cells. T15 – restimulated control, TNT – co-culture. **(b)** The AXL IHC staining in ccRCC primary tumor. The arrowhead indicates the AXL positive staining in TILs. P1-P3 – tumor stage. **(c and d)**The percent of stained cells considering: C - grading and D – staging; *n = 161*, magnification 400x.

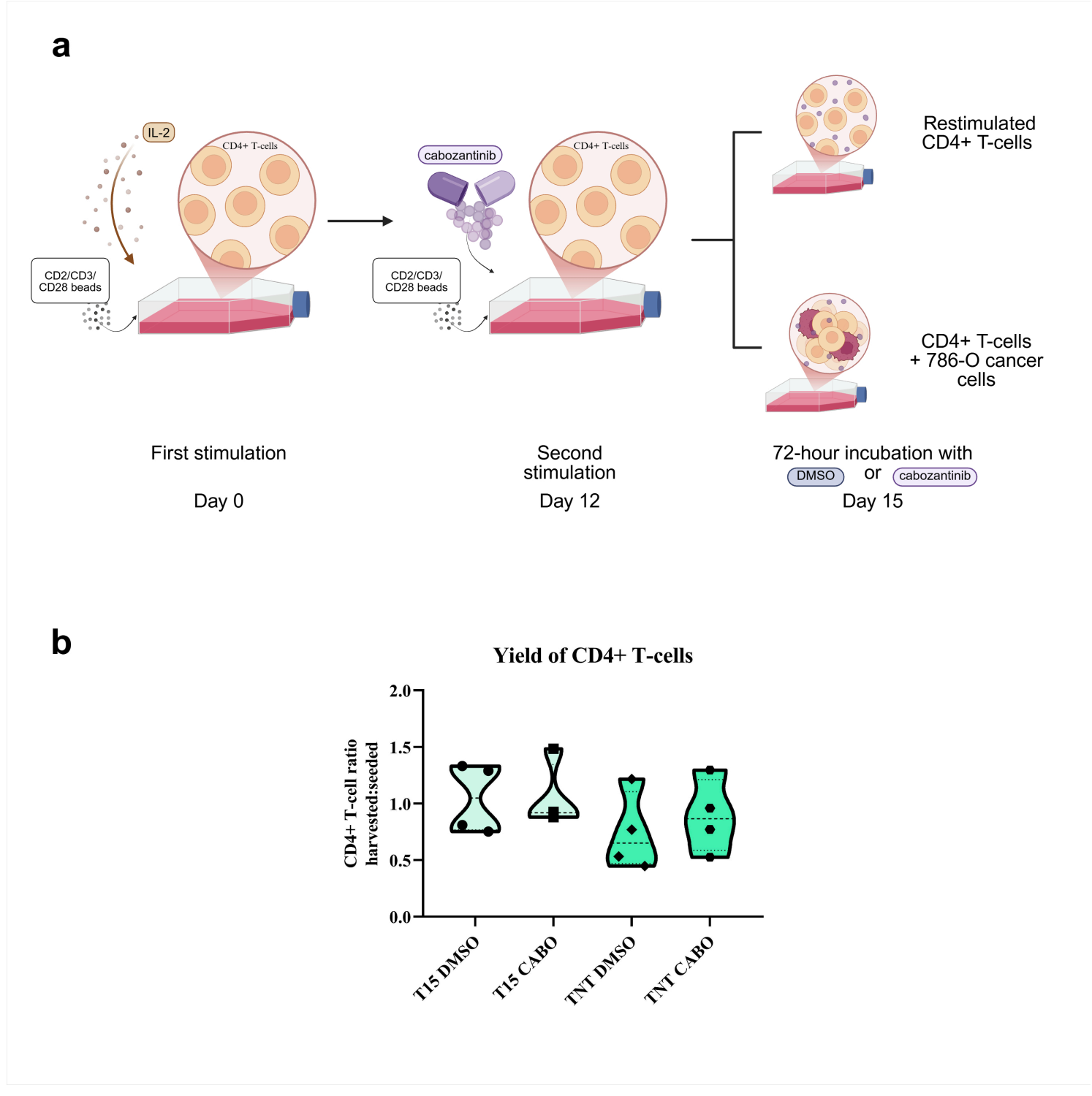


Figure 2

Experimental design and effect of cabozantinib on CD4+ T-cell yield. (a) Schematic diagram of CD4+ T-cell exhaustion experiment with cabozantinib supplementation at day 12**. (b)** Yield of CD4+ T-cells in control (DMSO) and treated (CABO) groups. No statistically significant differences were observed. Data represent mean ± SEM from *n = 4*biological replicates.

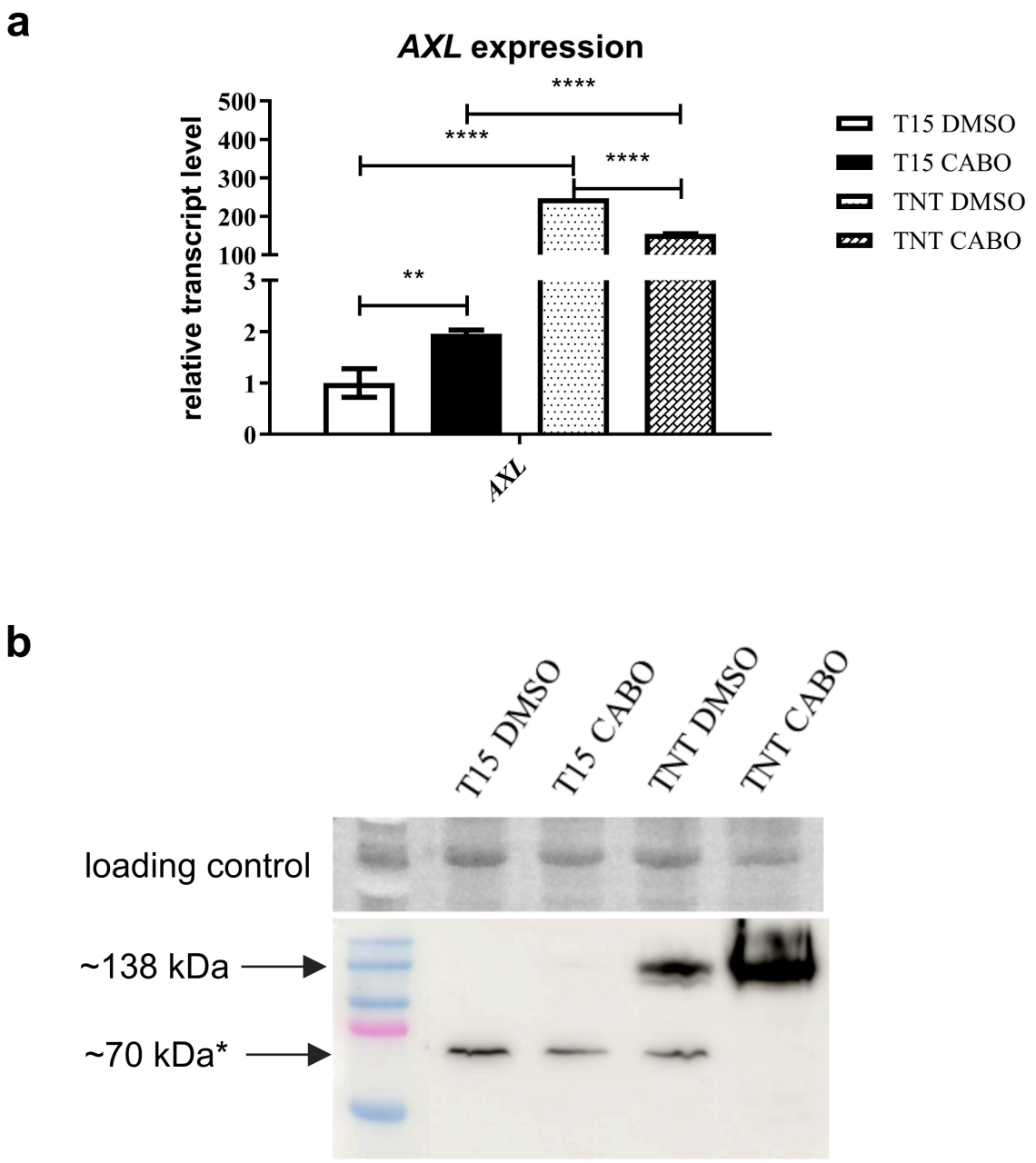


Figure 3

Cabozantinib alters the expression profile of exhaustion-associated markers. (a) Relative mRNA expression of PD-L2 (CD273), PD-L1 (CD274) and PD-1 (CD279) in CD4+ T-cells. Two-way ANOVA with post hoc Tukey's correction was used for statistical analysis (**** < 0.0001, *** < 0.001, ** < 0.01, * < 0.05); *n = 3*. **(b)** Western blot analysis of PD-L2, PD-L1 and PD-1 protein expression on CD4+ T-cells with TCE staining as protein loading control. (**c)** FACS analysis of surface PD-1 and PD-L1 receptors after 72 hours of drug treatment. (**d)** Number of PD-1- and PD-L1-positive CD4+ T-cells in T15 and TNT groups

after cabozantinib treatment; *n = 4*. **(e)** Median fluorescence intensity of PD-1 and PD-L1 markers on CD4+ T-cell surface; *n = 4*.

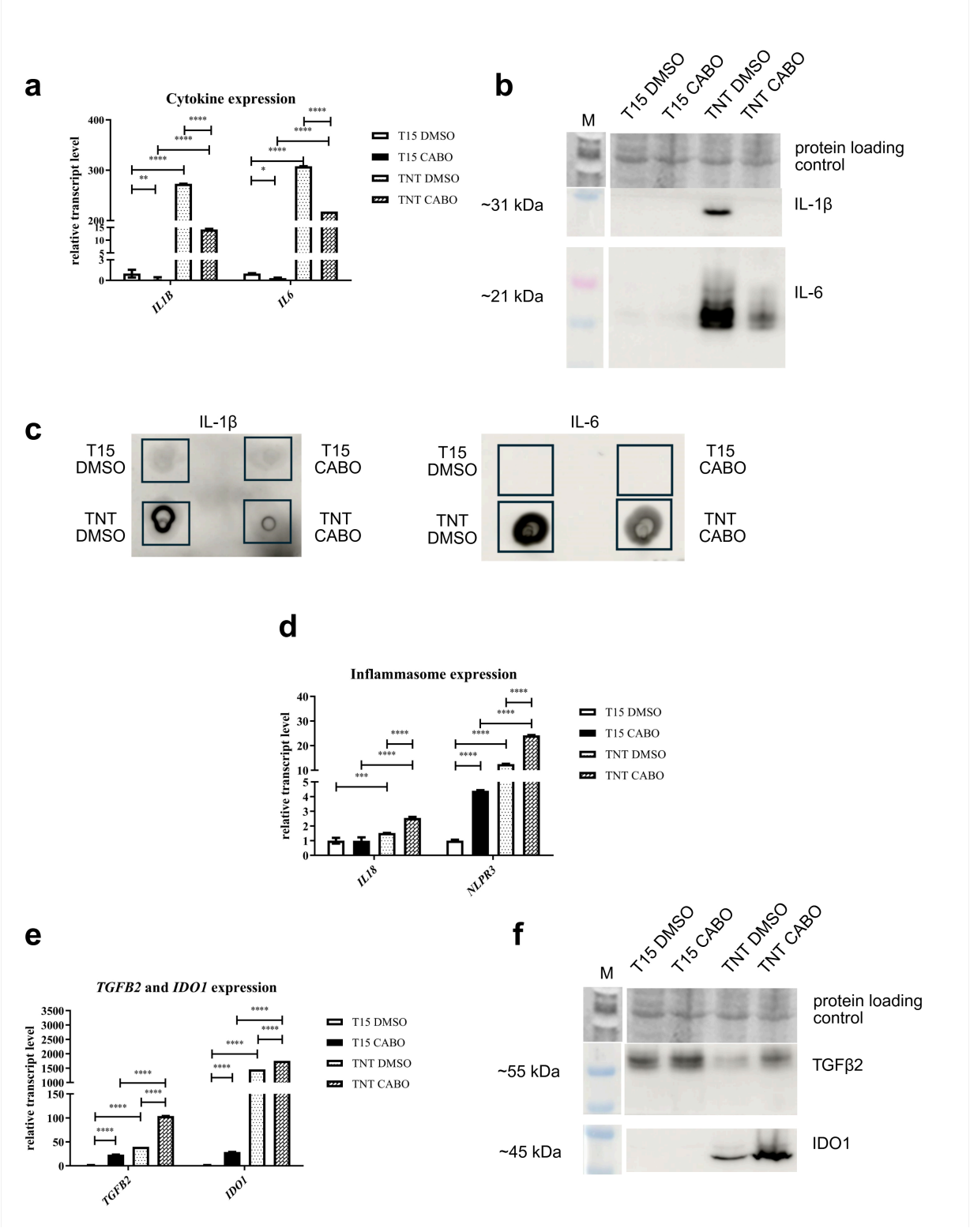


Figure 4

AXL is robustly induced in tumor-conditioned, exhausted CD4+ T-cells. (a) Relative AXL mRNA expression in CD4+ T-cells after 72h culture under the indicated conditions. Data normalized to T15

DMSO and reference gene UBC. Ordinary one-way ANOVA was used for statistical analysis (**** < 0.0001, *** < 0.001, ** < 0.01, * < 0.05); *n = 3*. **(b)** Representative Western blot analysis of AXL protein expression in CD4+ T-cell lysates. The predominant isoform 1 (~138 kDa) and a lower molecular weight isoform 3 (~70 kDa) are indicated.T15 = T-cells alone; TNT = T-cells co-cultured with 786-O tumor cells; DMSO - control; CABO – cabozantinib.

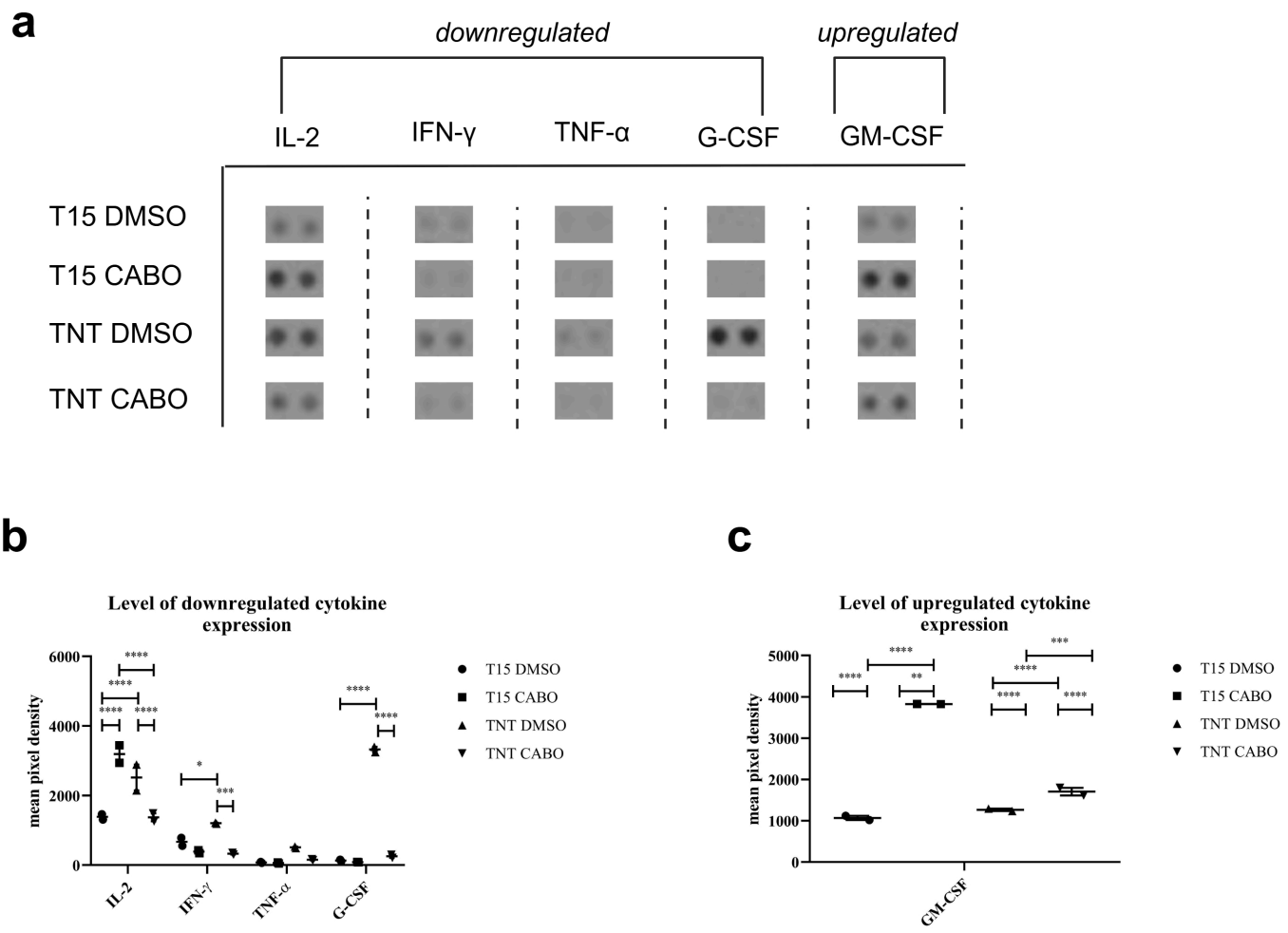


Figure 5

Effect of cabozantinib treatment on IL-1β, IL-6 expression in connection with inflammasome abundance and TGFβ2, IDO1 immunosuppressive factor expression levels. Cabozantinib downregulated the relative mRNA level **(a)** and protein level **(b)** of IL-1β and IL-6 cytokines. (c) Dot blot performed on the supernatants collected from each experimental group. (**d)** Relative transcript level of inflammasome specific genes were upregulated after treatment. Higher expression of immunosuppressive agents was observed both on mRNA (**e**) and protein level (**f**) after cabozantinib supplementation. Two-way ANOVA with post hoc Tukey's correction was used for statistical analysis (**** < 0.0001, *** < 0.001, ** < 0.01, * < 0.05); *n = 3*.

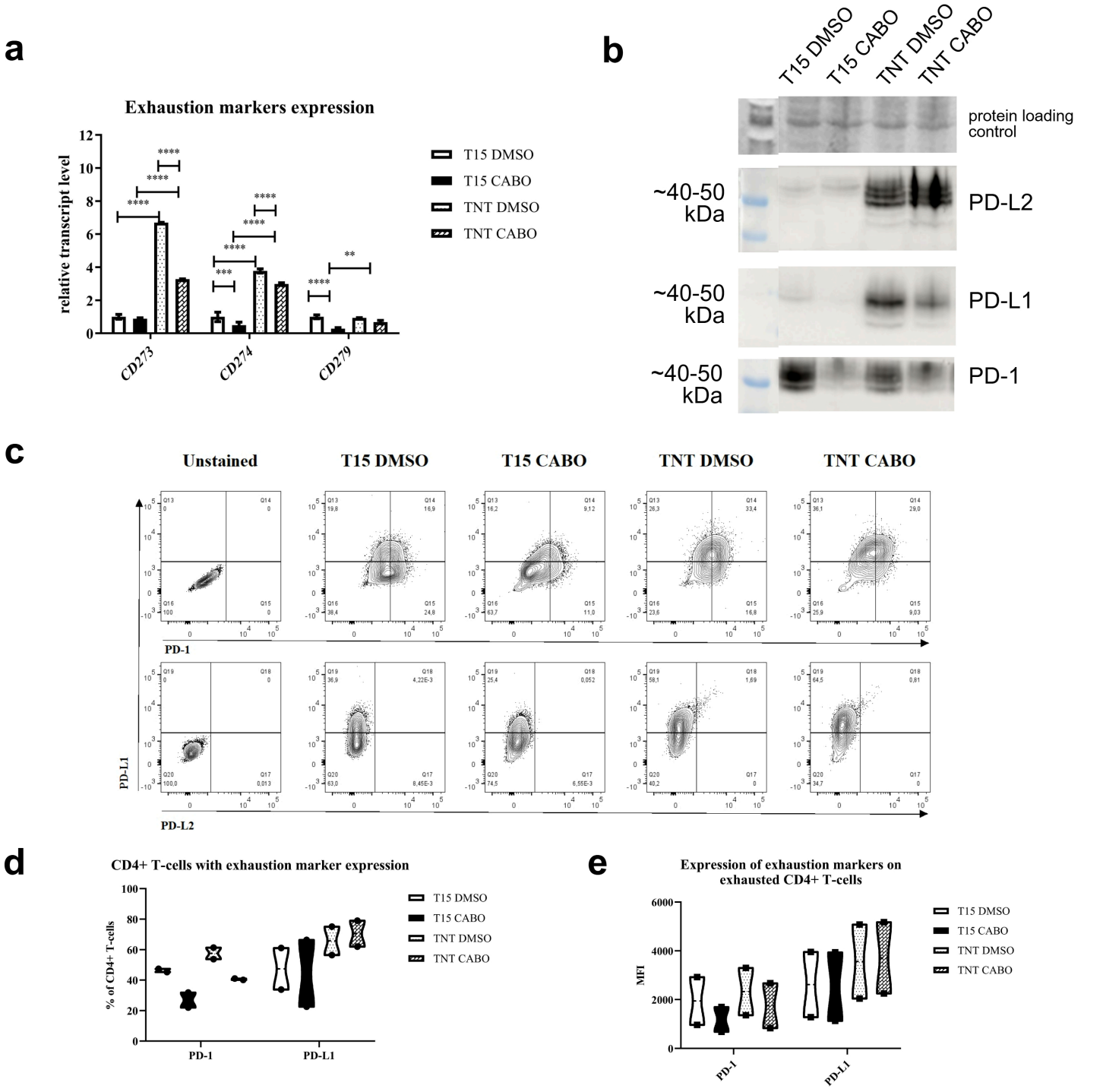


Figure 6

Extracellular cytokine profile after cabozantinib treatment of CD4+ T-cells. (a) Dot blot figures showed differences in expression of IL-2, IFN-γ, TNF-α, G-CSF and GM-CSF cytokines. Mean pixel density of downregulated **(b)** and upregulated **(c)** cytokines. Two-way ANOVA with post hoc Tukey's correction was used for statistical analysis (**** < 0.0001, *** < 0.001, ** < 0.01, * < 0.05), *n = 3*.

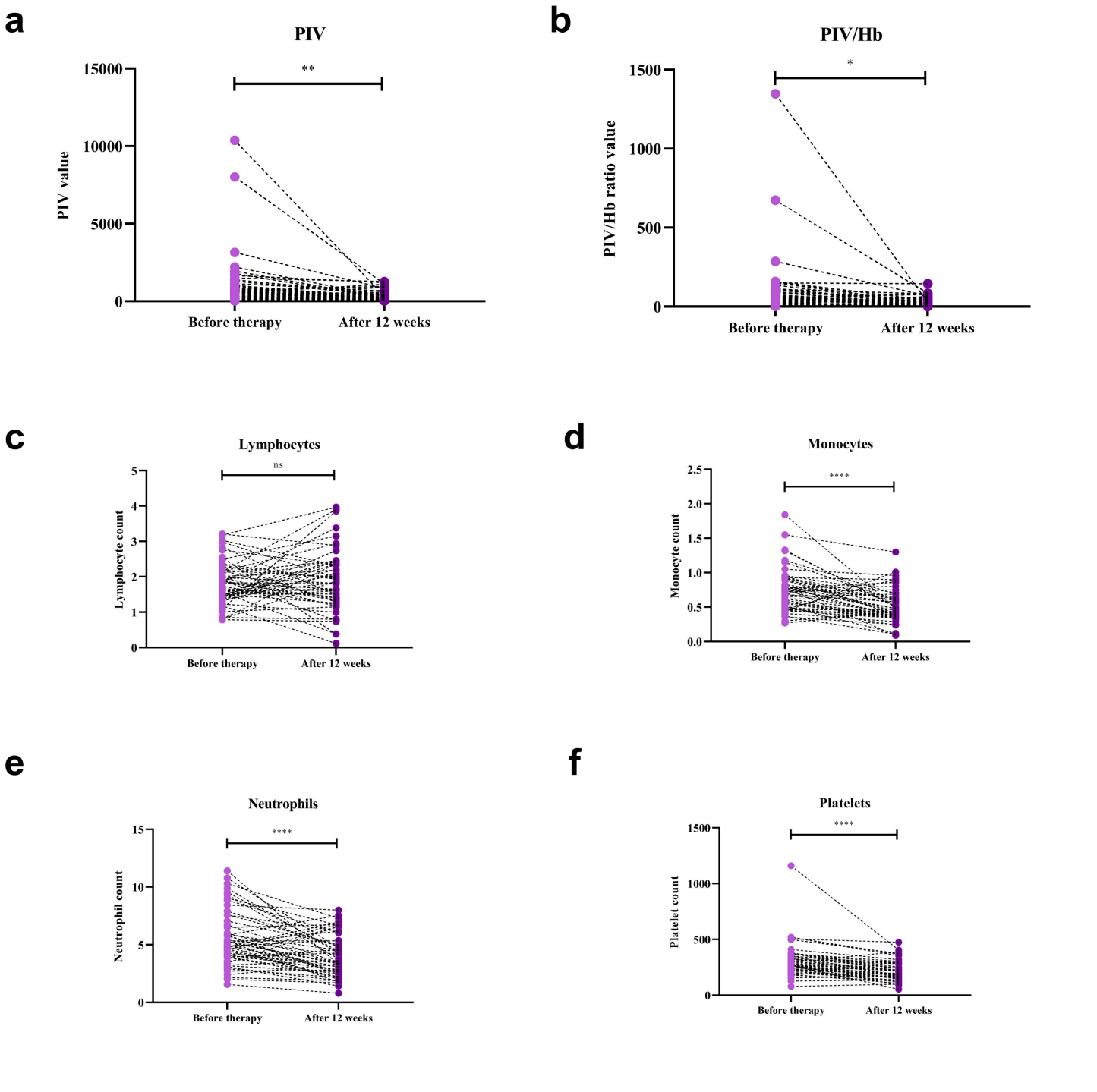


Figure 7

Pan-immune inflammation value and complete blood count were calculated comparing baseline and 12-week treatment levels. (a) PIV value**; (b)** PIV divided by hemoglobin level; **(c)**Lymphocyte count; **(d)** Monocyte count; **(e)** Neutrophil count; **(f)**Platelet count. Paired t test was used for statistical analysis (**** < 0.0001, *** < 0.001, ** < 0.01, * < 0.05), *n = 55*.

Supplementary Files

This is a list of supplementary files associated with this preprint. Click to download.

- SupplementaryDataS1.pdf
- SupplementaryDataS2.pdf
- SupplementaryDataS3.xlsx